



## Research Paper

# Association between brain morphology and electrophysiological features in Congenital Zika Virus Syndrome: A cross-sectional, observational study

Eduardo B Sequerra<sup>a</sup>, Antonio J Rocha<sup>a</sup>, Galtieri O C de Medeiros<sup>b</sup>, Manuel M Neto<sup>b</sup>,  
 Claudia R S Maia<sup>c</sup>, Nívia M R Arrais<sup>c</sup>, Mylena Bezerra<sup>c</sup>, Selma M B Jeronimo<sup>d,e</sup>,  
 Allan Kardec Barros<sup>f</sup>, Patrícia S Sousa<sup>a,f</sup>, Aurea Nogueira de Melo<sup>c</sup>, Claudio M Queiroz<sup>a,\*</sup>

<sup>a</sup> Brain Institute, Federal University of Rio Grande do Norte, 59056-450 Natal, RN, Brazil

<sup>b</sup> Imaging Diagnostic Center, Onofre Lopes University Hospital, Federal University of Rio Grande do Norte, 59012-300 Natal, RN, Brazil

<sup>c</sup> Department of Pediatrics, Onofre Lopes University Hospital, Federal University of Rio Grande do Norte, 59012-300 Natal, RN, Brazil

<sup>d</sup> Institute of Tropical Medicine of Rio Grande do Norte, Federal University of Rio Grande do Norte, 59056-450 Natal, RN, Brazil

<sup>e</sup> National Institute of Science and Technology of Tropical Diseases, Natal, RN, Brazil

<sup>f</sup> Department of Electrical Engineering, Federal University of Maranhão, 65080-040 São Luís, MA, Brazil

## ARTICLE INFO

## Article History:

Received 31 January 2020

Revised 30 July 2020

Accepted 30 July 2020

Available online 27 August 2020

## Keywords:

Epilepsy  
 Hypsarrhythmia  
 Sleep spindles  
 Infants  
 Microcephaly

## ABSTRACT

**Background:** Intrauterine infection with the Zika virus (ZIKV) has been connected to severe brain malformations, microcephaly, and abnormal electrophysiological activity.

**Methods:** We describe the interictal electroencephalographic (EEG) recordings of 47 children born with ZIKV-derived microcephaly. EEGs were recorded in the first year of life and correlated with brain morphology. In 31 subjects, we tested the association between computed tomography (CT) findings and interictal epileptiform discharges (IED). In eighteen, CTs were used for correlating volumetric measurements of the brainstem, cerebellum, and prosencephalon with the rate of IED.

**Findings:** Twenty-nine out of 47 (62%) subjects were diagnosed as having epilepsy. Those subjects presented epileptiform discharges, including unilateral interictal spikes (26/29, 90%), bilateral synchronous and asynchronous interictal spikes (21/29, 72%), and hypsarrhythmia (12/29, 41%). Interestingly, 58% of subjects with clinical epilepsy were born with rhombencephalon malformations, while none of the subjects without epilepsy showed macroscopic abnormalities in this region. The presence of rhombencephalon malformation was associated with epilepsy (odds ratio of 34; 95% CI: 2 - 654). Also, the presence of IED was associated with smaller brain volumes. Age-corrected total brain volume was inversely correlated with the rate of IED during sleep. Finally, 11 of 44 (25%) subjects presented sleep spindles. We observed an odds ratio of 0.25 (95% CI: 0.06 - 1.04) for having sleep spindles given the IED presence.

**Interpretation:** The findings suggest that certain CT imaging features are associated with an increased likelihood of developing epilepsy, including higher rates of IED and impaired development of sleep spindles, in the first year of life of CZVS subjects.

**Funding:** This work was supported by the Brazilian Federal Government through a postdoctoral fellowship for EBS (Talented Youth, Science without Borders), an undergraduate scholarship for AJR (Institutional Program of Science Initiation Scholarships, Federal University of Rio Grande do Norte, Brazil), by International Centre for Genetic Engineering and Biotechnology (CRP/BRA18-05\_EC) and by CAPES (Grant number 440893/2016-0), and CNPq (Grant number 88881.130729/2016-01).

© 2020 The Authors. Published by Elsevier Ltd. This is an open access article under the CC BY-NC-ND license. (<http://creativecommons.org/licenses/by-nc-nd/4.0/>)

**Abbreviations:** ZIKV, Zika virus; HC, head circumference; TORCH, toxoplasmosis, rubella, cytomegalovirus, and herpes simplex virus; SWD, spike and wave discharges; ROI, region of interest; CZVS, Congenital Zika Virus Syndrome

\* Corresponding author.

E-mail address: [clausqueiroz@neuro.ufrn.br](mailto:clausqueiroz@neuro.ufrn.br) (C.M. Queiroz).

## 1. Introduction

Brazil registered thousands of microcephaly cases associated with congenital Zika virus (ZIKV) infection during the 2015 outbreak [1]. Brain abnormalities were highly diverse among affected subjects and included cell migration defects, multiple and diffuse calcifications, an overall decrease in the encephalic volume, and enlargement of the ventricles [2-5]. These severe central nervous system malformations

## Research in context

### Evidence before this study

Since the outbreak of microcephaly associated with congenital ZIKV infection in 2015–2016, different studies focused on describing morphological alterations in the brain or EEG abnormalities. We searched PubMed for all articles describing anatomical and physiological alterations in ZIKV-derived microcephaly up to April 2020. Description of the brain morphology revealed a wide diversity of structural abnormalities, from the often-present neuronal migration defects to the less frequent malformation of the rhombencephalon. EEG recordings revealed varied epileptiform discharges in a subset of subjects. However, none of those studies performed quantitative analysis on the morphological and electrophysiological data nor tried to establish correlations between them.

### Added value of this study

We report the EEG and computed tomography findings of a cross-sectional cohort of subjects with ZIKV-derived microcephaly. We observed that the occurrence of rhombencephalon malformations is strongly associated with epilepsy. Moreover, by performing volumetric analysis, we determine that subjects with IEDs have lower brain volume, and its magnitude is inversely correlated with the rate of discharges. We also observed that the expression of sleep oscillations, i.e., sleep spindles, is impaired in the presence of epileptiform discharges and rhombencephalic malformations.

### Implications of all the available evidence

Infants with ZIKV-derived microcephaly commonly present irritable behavior, which may develop into subclinical and clinical seizures. Identifying signs with predictive power over clinical evolution can help the physician to determine better treatment and, consequently, prognosis. The present study reports that clinical cases with severe malformations of the rhombencephalon and reduced total brain volume have a higher chance of also showing pathological brain activity, including epileptiform discharges and reduced sleep-related oscillations.

describing brain activity in ZIKV-induced malformations. Here, we present insightful correlations between the occurrence of epileptiform discharges and rhombencephalon malformations, prosencephalon volume and sleep-related oscillations, which can help manage the disorder.

## 2. Materials and methods

### 2.1. Study design and participants

After the start of the microcephaly outbreak in the state of Rio Grande do Norte, northeast Brazil, the Federal University of Rio Grande do Norte became one of the reference centers for assessment of cases. Prior to the ZIKV outbreak, the definition of microcephaly was solely based on head circumference (HC; HC < 33 cm were included in the reports) [16]. This sensitivity threshold was later reduced to 32 cm in December 2015 [17], and adjustments were made to correct for gender and gestational age at birth according to World Health Organization (WHO) guidelines [18,19]. Therefore, a cut-off point of 2 standard deviations below the WHO reference for term neonates and the intergrowth reference for pre-term neonates were used [20]. Those criteria yielded 73 cases of suspected ZIKV infection associated with microcephaly between May 2015 and October 2016 (Fig. 1). Later, confirmation procedures revealed two cases of microcephaly *vera* and one premature newborn who was erroneously included in the initial cohort. Routine EEG recordings were made in 47 subjects, while no EEG information could be retrieved in the remaining 23. Thirty-one out of the 47 included subjects underwent computer tomography (CT), and among 18 of these 31, the exam allowed volumetric reconstruction of the brain that was used for the correlational study (Fig. 1). Of the 47 included subjects, the serologic analysis confirmed the presence of anti-ZIKV antibodies by ELISA (Euroimmun, Lübeck, Germany, or Meridian Bioscience, Memphis, USA) in the maternal blood of 31 mothers. Nine of these 31 children were also positive for ZIKV. Cases where the serological diagnosis was not available, but the mother or any other family members reported having experienced at least one symptom of ZIKV viremia, were classified as probable ( $N = 9$ ; see supplementary Table 1). In the remaining 7 cases, the information about maternal symptoms was missing, or the mother reported having no symptoms of arbovirus infection. In those cases, individuals were classified as suspected. Tests for other infectious diseases associated with microcephaly (TORCH: Toxoplasmosis, Rubella, CMV, and Herpes; supplementary Table 1) showed that 34% of the mothers had previously been exposed to toxoplasmosis and 40% to cytomegalovirus (in both cases, IgG+ and IgM-). None of them had a recent response (IgM+) to TORCHs.

### 2.2. EEG recordings and analysis

Recordings were made using an adapted version of the International 10–20 system and a digital EEG unit (EEG-1200, Nihon-Kohden, Tokyo, Japan) with a bipolar longitudinal derivation with 18 electrodes (see supplementary material for details; Fig. 3A). In most cases, the session started while the child was still awake (fully or drowsy) and progressively transitioned from waking to sleep state. Of the recordings, 41 were performed during spontaneous sleep, 3 had pharmacologically induced sleep (chloral hydrate 20%), and 3 did not sleep. Two experienced pediatric neurologists (ANM and PSS) and one experimental neurophysiologist (CMQ) blindly and independently analyzed the EEG recordings. While the former produced a validated medical report for diagnostic purposes, the latter concentrated on extracting global and local features of the signals, including morphology, occurrence, localization and duration of epileptiform discharges and sleep-related oscillations. Those variables were correlated with brain morphology findings. Recordings from children

are thought to be due to ZIKV tropism for neural cells [6], where it promotes mitochondrial oxidative stress and cell death [7].

Brain malformations resulting from infections have been associated with epileptiform discharges. Congenital cytomegalovirus (CMV) infection induces microcephaly and seizures in 83% of the cases [8]. In those subjects, seizures usually start at 3–9 months after birth, and behavioral signs do not necessarily occur in association with electroencephalographic (EEG) epileptiform activity [9]. Congenital syphilis and toxoplasmosis also lead to EEG abnormalities, including hypsarrhythmia [10]. Recent reports described that ZIKV infection during pregnancy could also lead to seizures and epilepsy in approximately half of the cases [11,12].

Despite many of the clinical presentations of the Congenital Zika Virus Syndrome (CZVS) having been described so far [13], few studies attempted to portray the electrophysiological patterns associated with ZIKV-induced microcephaly and brain volume [11,12,14]. No study has quantified physiological brain oscillations, such as those observed during sleep, or its relation to pathological brain activity. Although data are still lacking on whether routine EEG in a child with microcephaly can improve diagnosis and treatment [15], previous observations suggest that EEG recordings may be a valuable tool for

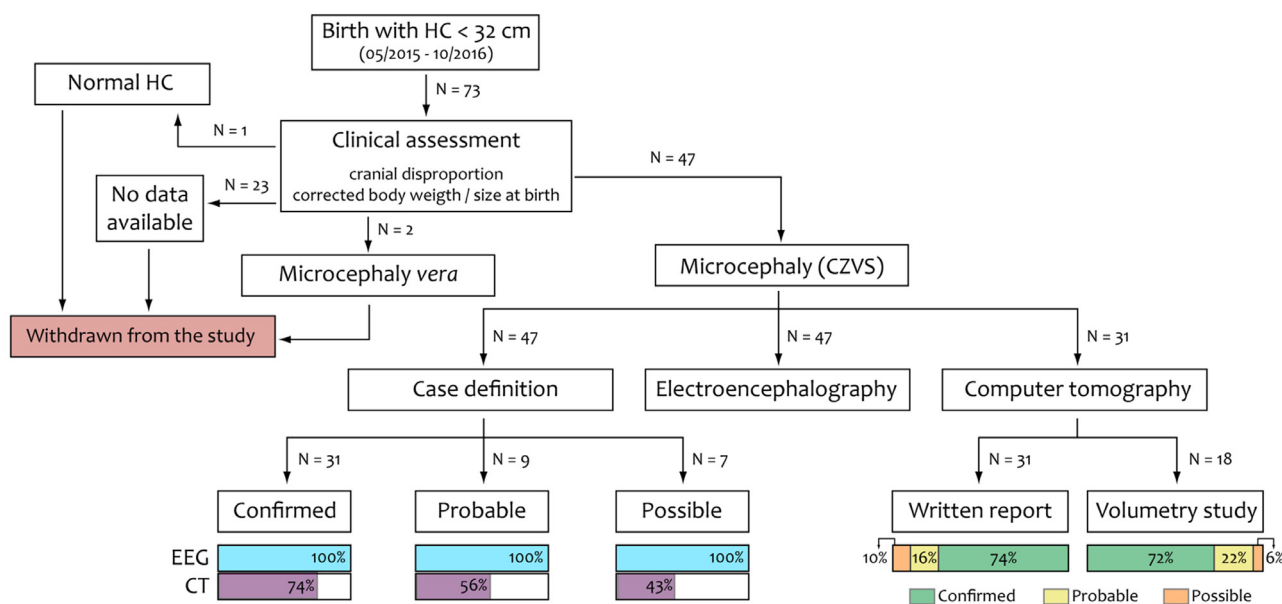


**Fig. 1.** Flowchart of the cohort of microcephaly cases enrolled in the study. After clinical assessment, subjects were included in the Brazilian protocol for microcephaly and underwent serological, electrophysiological, and imaging exams. The number of subjects (N) varied in each step, and the number of overlapping exams is shown at the bottom. HC: head circumference.

younger than four months showed considerable amplitude attenuation without sustained or transient oscillations and were excluded from further analysis.

### 2.3. Computerized tomography imaging and volumetric analysis

Children were scanned in computerized tomography (Philips Brilliance 64; Philips Medical Systems; Cleveland, USA) as previously reported [4]. An expert radiologist (MMN) used CT images to score (present or absent) eleven brain morphological attributes. Brain region volumes were determined by another author (GOCM) using software Advantage Workstation 4.6 (General Electric Healthcare). Briefly, brain tissue was selected by eliminating bone tissue through the selection of regions with pixels with more than 62 Hounsfield Units. Small calcification points were eliminated from the brain tissue even though their presence did not interfere with the calculation of the brain volume. Areas with liquor were removed and corresponded to equal or lower than selected region of interest (ROI) with ventricles (magnitude varied between 0 and 20 Hounsfield Units per pixel). Each brain region was determined by manual contouring using the axial, sagittal, and coronal orientations. We used interpolation to render the volumetric contour between manually drawn CT slices (supplementary video 1) and to extract estimations of the brainstem, cerebellum, and prosencephalon volumes. Both imaging experts were blind to the clinical diagnosis and the electrophysiological profile.

### 2.4. Statistical analysis

The information about the clinical evaluation available for all 47 children was collected by the physician authors (CRSM, NMRA, MB, SMBJ, ANM), presented in supplementary Table 1. Pearson correlation method was used for determining the strength of the relationship between pairs of variables (HC and interictal spike rate vs. regional brain volumes). Correlation analysis included only subjects with both variables (subjects with missing values were not included). Since brain image acquisition was performed in children at different ages ( $64 \pm 83$  days-old, standard deviation,  $N = 18$ ; supplementary Fig. 4B), we normalized their brain volumes using a linear regression model that relates brain growth rates and postnatal period in the first

three months of age of normocephalic children [21]. We used unpaired *t*-test (Welch correction) to compare HC at birth, growth of HC in the first year of life, gestational week at birth, gestational week of the reported symptoms between subjects with and without epilepsy/interictal epileptiform discharges (IED). Association between dichotomous categorical variables was calculated using Fisher's Exact Test and Jaccard's Index of Similarity (JIS) [22]. Principal Component Analysis (PCA) and binary logistic regression were used to further test the redundancy of brain morphological variables and to model the probability of having epilepsy/IED, respectively (see Supplementary Information). The odds ratio was computed using Haldane-Anscombe correction when one of the groups had zero entries. Confidence intervals (when possible, groups  $\geq 5$ ) and statistical significance were set at 95% and 5%, respectively. Statistical analyses were performed using Prism (GraphPad) and Matlab (Mathworks).

### 2.5. Ethical considerations

The study protocol was registered at Plataforma Brasil (<http://plataformabrasil.saude.gov.br/login.jsf> CAAE numbers: 57444016.1.0000.5292 and 53111416.7.0000.5537), and reviewed and approved by the Ethics Committee of the Federal University of Rio Grande do Norte. All parents or the legal guardian reviewed and signed the informed consent on behalf of the subjects authorizing the use of their routine exams for investigation purposes.

### 2.6. Role of the funding source

The funding agencies had no influence on study design, data collection and analysis. The corresponding author had full access to the data and is responsible for the decision of submitting for publication.

## 3. Results

### 3.1. Clinical data

We analyzed EEG recordings from 47 children diagnosed with microcephaly in the state of Rio Grande do Norte, Brazil, during the first ZIKV outbreak in the second semester of 2015 (Fig. 2A). Twenty-

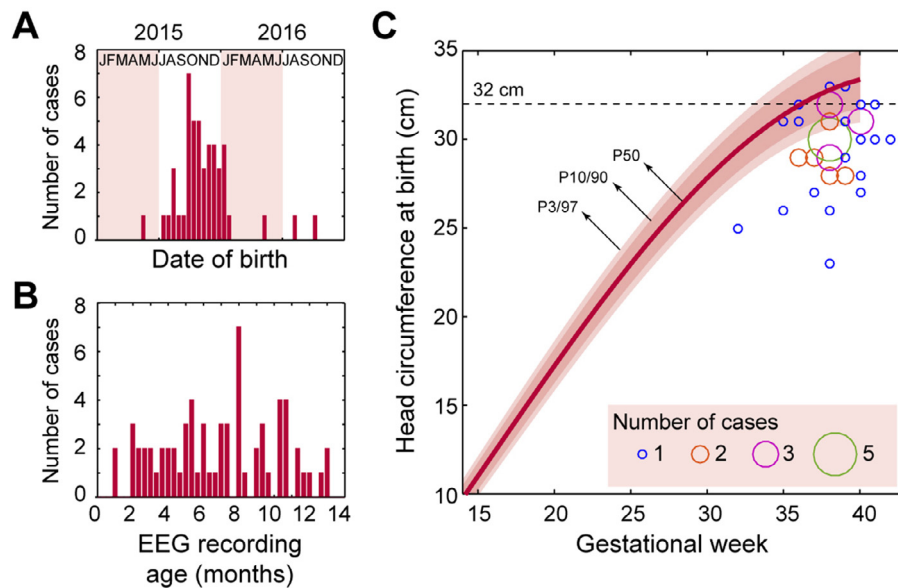


**Fig. 2.** Date of birth, age at EEG recordings and head circumference at birth. (A) Histogram showing the distribution of the birth dates for all microcephaly cases included in the present study ( $N = 47$ ). (B) Histogram showing the subjects' age at the time of the EEG recordings used in this study ( $N = 67$ ). Most of the subjects were recorded only once (one EEG session: 72%; two: 15%; three: 9%; four: 2%). (C) Correlation between gestational week and HC at birth as reported by primary care services (four missing values). The red line represents the median HC of healthy subjects [20], and the two lighter red areas represent percentiles 10–90 and 3–97. Most of the subjects showed HC at birth between 26 and 32 cm (mean  $\pm$  SEM:  $29.5 \pm 2.2$  cm). The majority of the newborns (84%) were considered term, although some premature babies were included. (For interpretation of the references to color in this figure legend, the reader is referred to the web version of this article.)

five were female. The average gestational week at birth was  $37.8 \pm 2.3$  weeks (Fig. 2B). Their average HC at birth was  $29.5 \pm 2.2$  cm, and the HC distribution as a function of the gestational age at birth is shown in Fig. 2C. Of importance, seven subjects included in this study had HC at birth equal to or higher than 32 cm. The subjects were included in this study after serological confirmation of ZIKV infection, imaging, clinical, neurological evaluation, and low HC for their age. EEGs were recorded at different ages ranging from four up to thirteen months (Fig. 2B).

### 3.2. Electroencephalographic abnormalities in Congenital Zika Virus Syndrome

During routine medical consultations at the outpatient service of the university hospital, epilepsy was diagnosed in 29 out of 47 subjects, according to ILAE guidelines [23]. Briefly, two or more unprovoked seizures were reported by family members or caregivers. Clinically, seizures started with recurring spasms and eventually evolve to tonic seizures, as recently reported [24,25]. As part of the medical evaluation, all subjects were referred to the Imaging Center of the university hospital for EEG investigation. Recordings occurred during spontaneous sleep ( $N = 41$ ), after induced sleep (chloral hydrate,  $N = 3$ ) or during awake ( $N = 3$ ). Sleepiness was assessed by the technician through direct observation of the child during the recording session. Additional signs of transition into sleep included the appearance of slow oscillations and reduced high-frequency activity from facial muscles in frontal EEG derivations (supplementary Fig. 1). The evaluation of the EEG recordings by an expert clinical neurophysiologist revealed that all subjects clinically diagnosed with epilepsy (29 out of 47) presented interictal epileptiform discharges (IED). At the time of EEG recordings, 12 out of 29, (41%) were under antiseizure medicine, including phenobarbital, valproic acid and vigabatrin (see supplementary Table 2).

The recordings revealed varied localized and generalized expressions of abnormal EEG activity (Fig. 3 and supplementary Fig. 2). Hypsarrhythmia was found in 25.5% of the cases ( $N = 12/47$ ; see supplementary Fig. 2A–C for hypsarrhythmia examples), unilateral spikes in 57.4% ( $N = 27/47$ ; Fig. 3B), bilateral spikes in 44.7% ( $N = 21/$

47; Fig. 3C), background asymmetry in 19.1% ( $N = 9/47$ ; supplementary Fig. 2D), diffuse low voltage attenuation in 38.3% ( $N = 18/47$ ), and high amplitude slow waves in 53.2% ( $N = 25/47$ ; supplementary Fig. 2E). Distinct patterns of spike and wave discharges (SWD) were observed, including bursts of SWD (Fig. 3D), SWD followed by suppression (supplementary Fig. 2F), localized (e.g., frontal) SWD (supplementary Fig. 2G) and SWD followed by theta waves ( $\sim 6$  Hz) in the occipital region (supplementary Fig. 2H). Usually, those events persisted throughout the recording session without behavioral signs unless the child awakened. Clinical seizures were rare, and only one event was observed in this dataset (Fig. 3E). Gestational week at birth ( $p = 0.9209$ ,  $t = 0.1002$ ,  $df=28$ ), gestational week of reported symptom ( $p = 0.0841$ ,  $t = 1.802$ ,  $df=24$ ,  $t$ -test with Welch's correction; Fig. 3F), or gender distribution ( $p = 0.5670$ , Chi-square=0.3277,  $df=1$ ) were not different between subjects with or without IED. Also, the HC at birth did not differ between these two groups ( $p = 0.1992$ ,  $t = 1.307$ ,  $df=38$ ; Fig. 3G).

### 3.3. Correlation between brain malformations and interictal epileptiform discharges

Thirty-one subjects had their cranial CT scored for macroscopic abnormalities (for the complete list of features evaluated refers to supplementary Table 1 and supplementary Fig. 3A). We used contingency analysis to determine whether morphological brain phenotype correlates with the presence of IED. Both the presence of calcifications in the thalamus and basal ganglia (Fisher's exact test;  $p = 0.0217$ , odds ratio=12.86 [95% CI: 1.27–130.60]), and periventricular calcifications (Fisher's exact test;  $p = 0.0317$ , odds ratio=6.88 [95% CI: 1.17–40.40]) were positively associated with IED. However, malformations in the prosencephalon, as defects of cortical gyrification and lateral ventricle dilation, were not. Of notice, those last two anatomical changes occurred in almost all subjects. Interestingly, all subjects presenting rhombencephalon atrophy (i.e., cerebellum and the brainstem) showed IED, while only 40% (8 out of 20) of the subjects where no clear macroscopic rhombencephalon malformations could be observed presented IED (Fisher's exact test;  $p = 0.0014$ , odds ratio=33.82 [95% CI: 1.75–654.80]; Fig. 4).

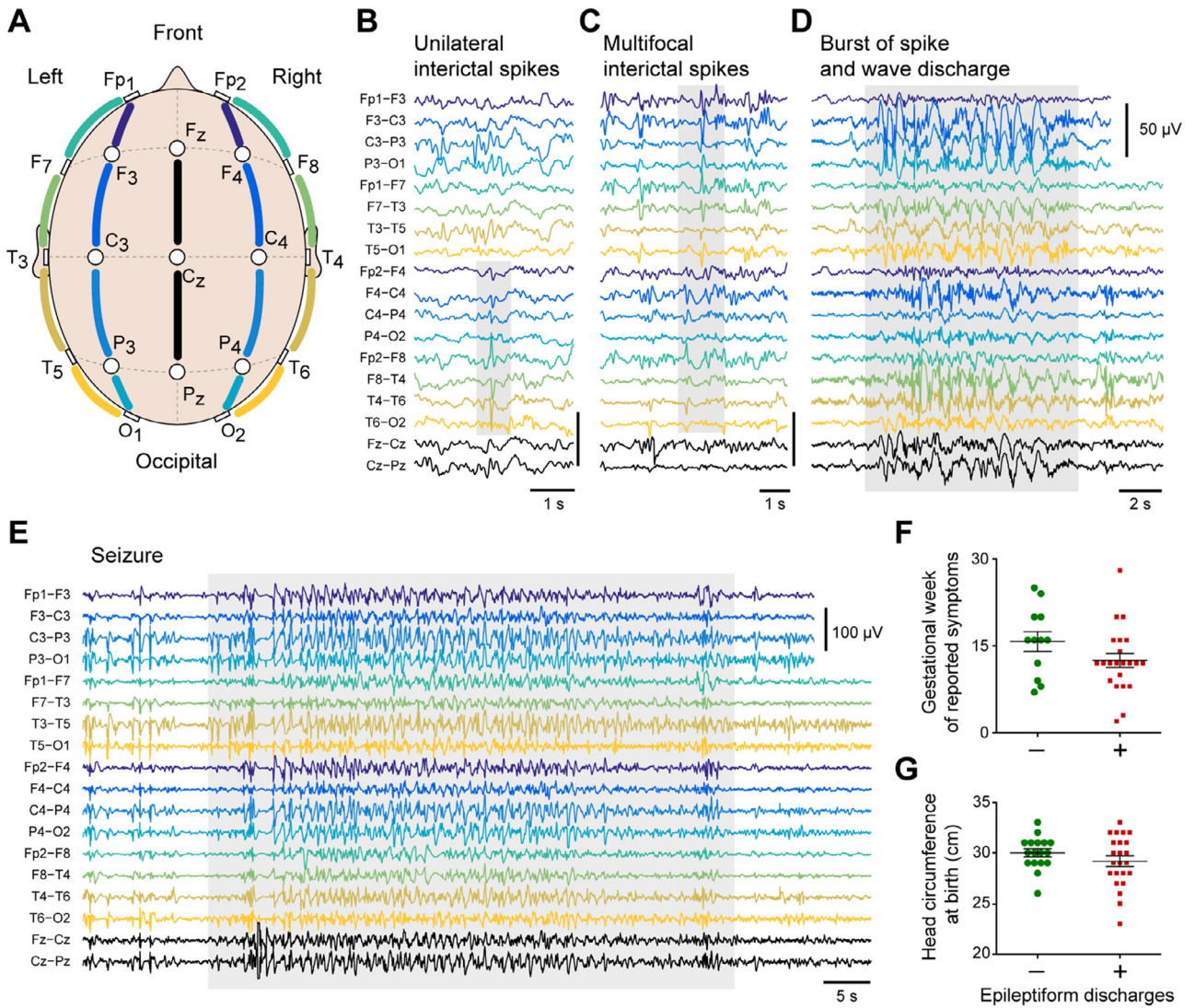


**Fig. 3.** Electroencephalographic abnormalities in Congenital Zika Virus Syndrome. (A) Color-coded illustration of the 10–20 head montage used and the bipolar derivations. (B–E) Representative examples of epileptiform discharges observed in our cohort where the shaded areas highlight one electrographic element. Epileptiform discharges included unilateral (B) and multifocal (C) interictal spikes, spike and wave discharges (D), and seizures (E). (F–G) Comparison of the gestational week of reported symptoms (F) and HC at birth (G) according to the expression of epileptiform discharge. No differences were observed in either comparison.

We further corroborated this conclusion using Jaccard's Similarity Index (supplementary Fig. 3B). This analysis showed that cerebellar and brainstem atrophies were positively associated, while pachygyria was negatively associated to lissencephaly, cranial misalignment, and brain cysts (supplementary Fig. 3B). This result suggests that brain malformations may be grouped in clusters with redundant and similar attributes. To test this hypothesis, we used the Jaccard's Index as a covariance matrix and performed PCA. The first nine components concentrate 95% of the explained variance (supplementary Fig. 3C). Vector projection of each attribute according to the first (22% of the explained variance) and second (18% of the explained variance) components show that malformations are not entirely redundant (supplementary Fig. 3D). For example, while pachygyria and lissencephaly are in opposed quadrants, cerebellar, and brainstem atrophies vectors point in the same direction. We then used logistic regression, a type of Generalized Linear Model (GLM), to determine which attribute better predicts the occurrence of IED. As shown in supplementary Table 3, calcification in the basal ganglia and thalamus, periventricular calcification, cerebellar and brainstem atrophies were the attributes most strongly associated with IED. Together, those results suggest that rhombencephalon atrophy, the presence of

calcifications in the basal ganglia, thalamus, and next to the lateral ventricles are associated with a higher chance of occurrence of epileptiform discharges in CZVS.

As our results showed a clear link between the occurrence of rhombencephalon malformations and IED, we tested the hypothesis whether these discharges are more likely observed in the most severe malformation cases (i.e., reduced brain mass) [21]. The corrected total brain volume at 90 days-old (supplementary Fig. 4A–C, see Methods) correlated with the HC at birth ( $R = 0.51$ ,  $p = 0.031$ ,  $N = 18$ ; supplementary Fig. 4D), suggesting that our correction method is robust. Averaging the corrected total brain volume in groups of subjects according to the presence of interictal spikes revealed an association between unilateral or bilateral spikes and hypsarrhythmia with reduced brain volumes (Fig. 5). Other abnormal activities (background asymmetry, diffuse low voltage, and high amplitude slow waves) were not associated with decreased brain volume (Fig. 5).

To further test the strength of this association, we computed the rate of interictal spikes in the first three principal components extracted from all EEG channels during the sleep episode (supplementary Fig. 5). We found the rate of interictal spikes negatively

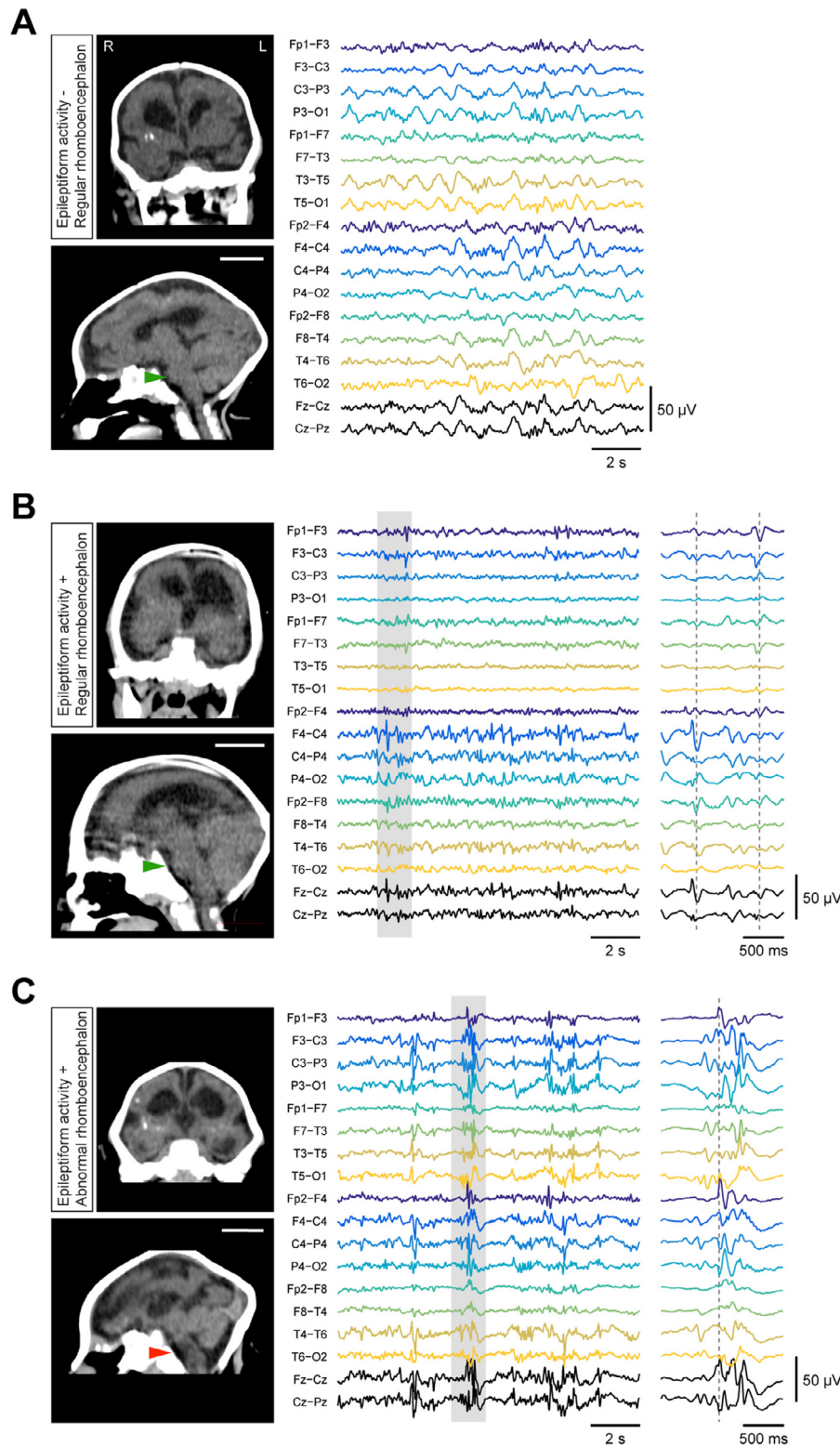


**Fig. 4.** Rhombencephalon malformation correlation with the occurrence of interictal epileptiform discharges. CT coronal (top) and sagittal (bottom) planes (left) and the corresponding EEG recordings (right) in subjects with regular rhombencephalon development (A and B, green arrows) and with brainstem and cerebellum atrophy (C, red arrow). Although subjects with no macroscopic rhombencephalon malformation can have epileptiform discharges (B), all the subjects with brainstem and cerebellum atrophy have epileptiform discharges (C). Note that the left cortical thinning in B is associated with reduced EEG amplitude in left hemisphere EEG electrodes. Shaded areas in B and C are magnified on the right traces, highlighting the diversity of electrographic events. Scale bars in CT images: 5 cm. Arrowheads point to the shape of the pons, significantly reduced in C. (For interpretation of the references to color in this figure legend, the reader is referred to the web version of this article.)

correlates with prosencephalic volume ( $R=-0.52$ ,  $p = 0.026$ ), but not with cerebellar ( $R=-0.05$ ,  $p = 0.821$ ) or brainstem ( $R=-0.16$ ,  $p = 0.510$ ) volumes (Fig. 6). Then, we used logistic regression to

determine the probability of having epilepsy based on the prosencephalon, cerebellum, or brainstem volumes (supplementary Fig. 6). This approach showed to be valuable in predicting lissencephaly

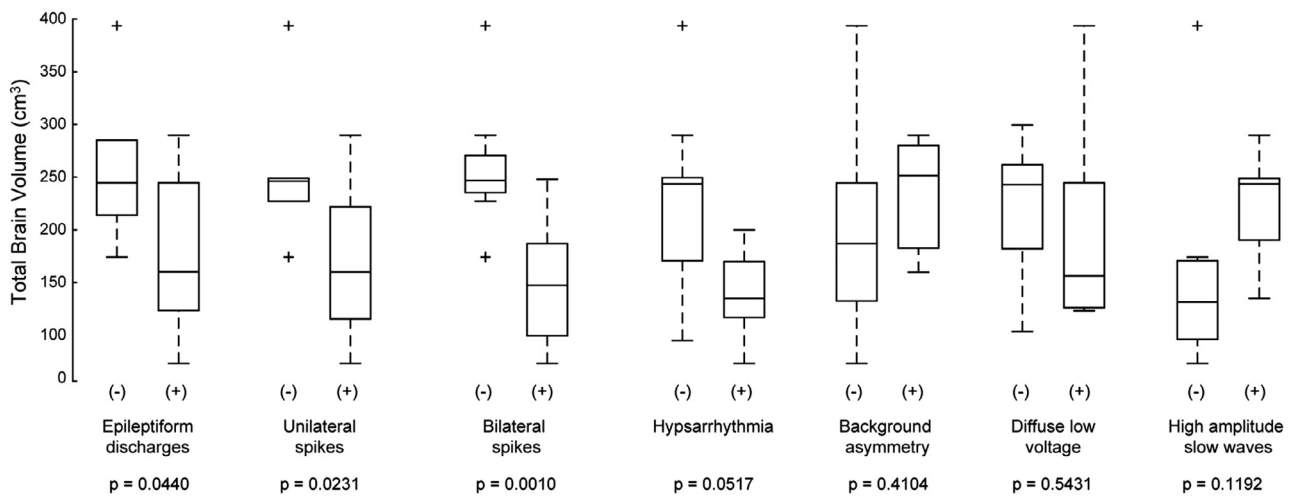


**Fig. 5.** Occurrence of interictal epileptiform discharges as associated with reduced brain volumes. Comparing the total brain volume (corrected for age) between subjects with different types of abnormal EEG activity revealed that unilateral, bilateral, and hypsarrhythmia are associated with reduced total brain volume, while background asymmetry, diffuse low voltage, and high amplitude slow waves are not.

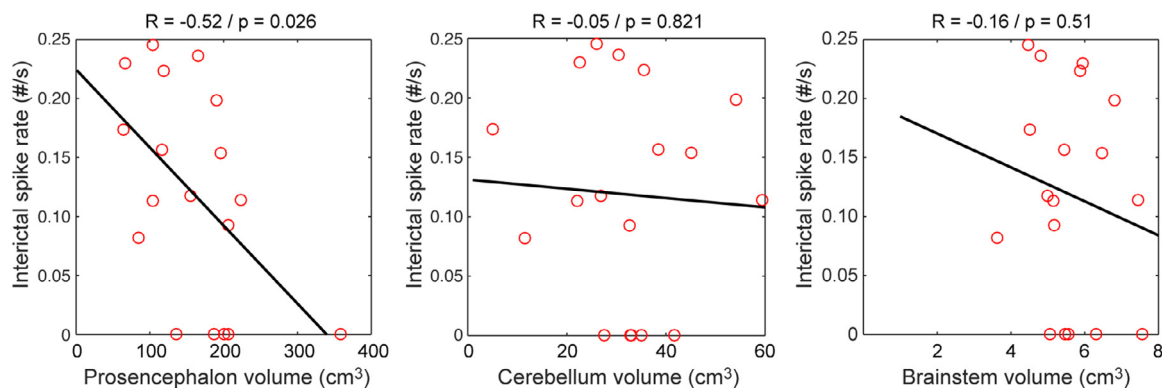


**Fig. 6.** Correlation between regional brain volumes and interictal spike rate during sleep. While the volume of prosencephalon is inversely correlated with the interictal spike rate (left), the volumes of the cerebellum (middle) and brainstem (right) are not.

based on the total brain volume (supplementary Fig. 6A) and cerebellar atrophy based on cerebellar volume (supplementary Fig. 6B). Total brain volume predicts the presence of epileptiform discharges in the EEG (supplementary Fig. 6C). The prosencephalon volume, but not cerebellar or brainstem volumes, predicts the occurrence of epileptiform discharges (supplementary Fig. 6D-F), which may result from the fact that the prosencephalon contributes to more than 80% of the total brain volume.

Finally, we computed the monthly increment of HC after birth for all subjects to determine whether postnatal growth could be associated with epileptiform discharges. We found no difference in cranial enlargement for subjects with and without epilepsy in the first year of life (supplementary Fig. 7). Those observations indicate that, along with the specific malformations described above, like the atrophy of rhombencephalic structures, the more accentuated loss of total brain and/or prosencephalic volume represent a higher risk for the development of epilepsy and IED.

#### 3.4. Impaired sleep spindles expression in Congenital Zika Virus Syndrome

We detected sleep spindles in 25% of the subjects ( $N = 11/44$  recordings with at least one sleep episode). Importantly, the age at the time of the EEG recording did not differ between subjects with and without spindles ( $177 \pm 20$  and  $195 \pm 20$  days-old, respectively;

Welch-corrected  $t = 0.6277$ ,  $p = 0.5345$ ,  $df=33$ ). Also, sleep spindles were less prevalent in those with epilepsy. While sleep spindles were detected in 7 out of 17 non-epilepsy subjects (41%), only 4 out of 27 epilepsy subjects (15%) showed this type of sleep oscillation (Fisher's exact test:  $p = 0.0754$ ). Synchronous spindles were observed in two subjects, one who did not show IEDs (Fig. 7A,B) and another with it (Fig. 7C,D). Averaged spectrograms, centered at the max spindle power, revealed a consistent 2-s, 12 Hz oscillations (Fig. 7B) with max energy in central electrodes (in this example, F3-C3 and F4-C4; asterisks in Fig. 7A). Fewer synchronous spindles, with reduced (relative) power, were detected in the epilepsy subject (Fig. 7D). Our algorithm automatically detected 1372 events from 13 subjects. Almost half of the detected events showed the highest power in frequencies around 6 Hz (Fig. 7E). Visual inspection of these events revealed a slower and irregular oscillation, in the theta-band, with a harmonic in the power spectrum within the spindle frequency (supplementary Fig. 8A). In one subject, these electrographic events could last longer (supplementary Fig. 8B), although most of them have ~2 s duration (supplementary Fig. 8C). The power of these detected events was higher at 7 and 11 Hz (Fig. 7G), with no difference between subjects with and without epilepsy (data not shown). The inter-spindle interval (a measure of spindle rate) was not different between epilepsy and non-epilepsy subjects (Fig. 7H), although spindles were shorter in the former (Fig. 7I). Theta oscillation (detected as a spectral harmonic of the true spindle) showed a similar duration

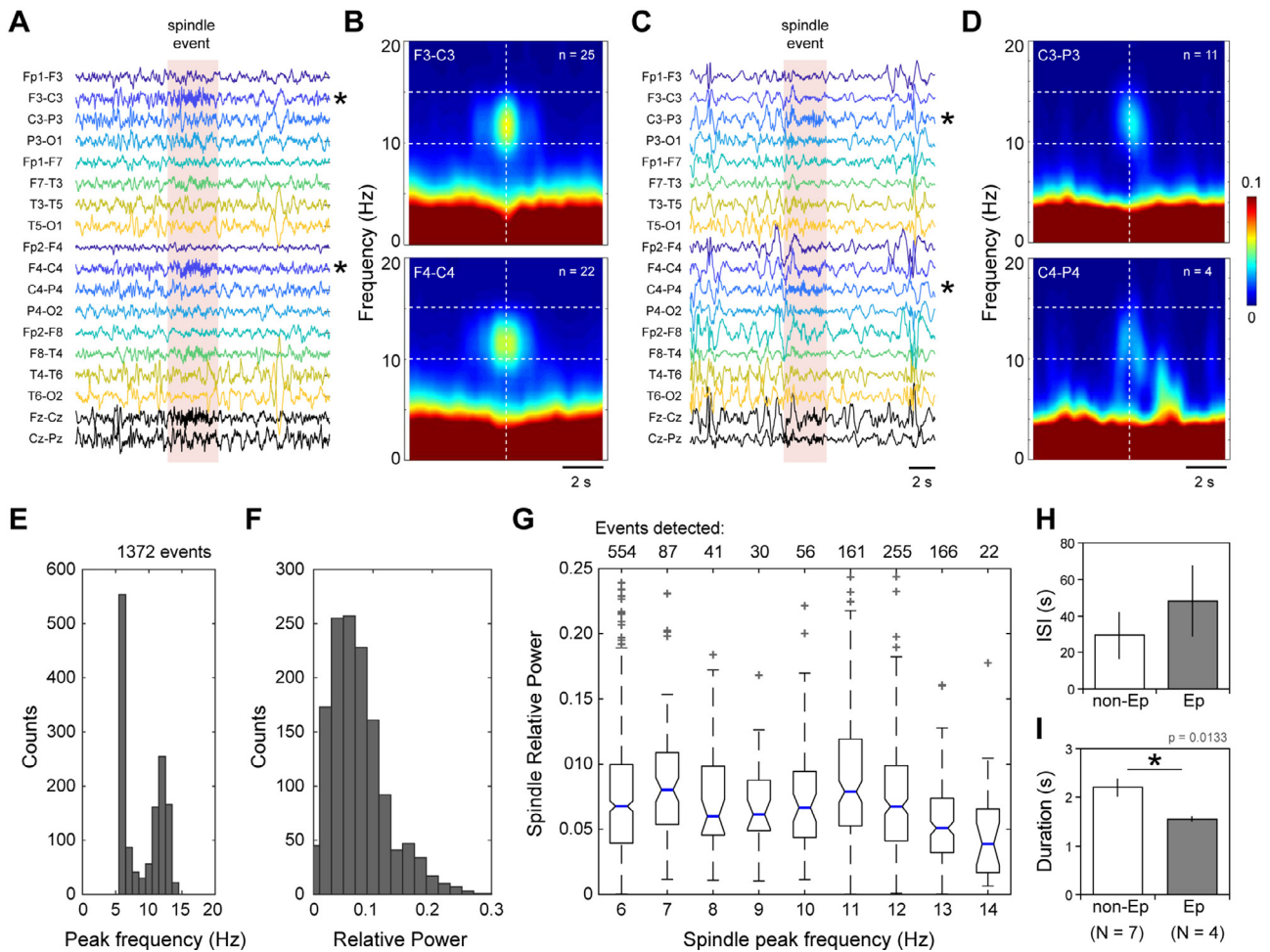


**Fig. 7.** Expression of sleep spindles is impaired in subjects with epileptiform discharges than in those without it. (A) A representative example of one synchronous and symmetrical sleep spindle (shaded area) in one non-epilepsy subject. (B) Averaged spectrograms (centered at the sleep spindle, vertical dashed line) of sleep spindles recorded in frontocentral electrodes (asterisks in A) showed high power at 12 Hz. (C) Representative example of one synchronous and symmetrical sleep spindle (shaded area) in one epilepsy subject. In this example, the electrodes with the highest power were shifted backward (i.e., in frontoparietal region). (D) In this subject, sleep spindles showed few detected events with reduced power. (E) Bimodal distribution of the sleep spindle peak frequency for all subjects and electrodes. (F) Distribution of sleep spindle relative power. (G) Boxplot of spindle relative power as a function of the power spectrum peak frequency. Note that most of the detected events show peak frequency of 6 Hz. (H) Inter-spindle interval (ISI), as a measure of sleep spindle rate, did not differ between non-epilepsy and epilepsy subgroups of subjects. (I) Sleep spindle duration was reduced in epilepsy subjects in comparison to non-epilepsy ones ( $p < 0.05$ , paired *t*-test). Data shows mean  $\pm$  S.E.M.

(supplementary Fig. 8D) and power (supplementary Fig. 8E) between epilepsy and non-epilepsy subjects. Interestingly, one subject in the epilepsy group showed clear unilateral spindle frequency decay (supplementary Fig. 9). While the left hemisphere (C3-P3) showed well-defined spindles, the right hemisphere regular spindles were usually followed by a theta oscillation (supplementary Fig. 9A). Individual analysis of these events showed that the intensity of this frequency decay varies significantly (supplementary Fig. 9B). Averaged spectrograms centered at the sleep spindle revealed the unilateral frequency decay (supplementary Fig. 9C). Finally, we found no association between the occurrence of sleep spindles and the growth of HC in the first year of life (supplementary Fig. 10). These observations suggest that the theta oscillation (with the frequency decay in one patient) might result from a corrupted sleep spindle generator network in subjects with epilepsy in CZVS.

#### 4. Discussion

It is now established that ZIKV infection during the gestational period can lead to severe developmental malformations, including microcephaly [1], cortical dysplasia [4], and retinal degeneration

[26]. Clinically, those subjects can show irritability, muscle spasms, hyperreflexia, and slow cognitive development [1]. The present study is the first to unveil correlations between quantitative morphological and electrophysiological (EEG) findings of CZVS. Surprisingly, although an abnormal neural tissue is a potential source for epileptiform activity, not all individuals with microcephaly develop epilepsy. Our analysis suggests that specific morphological characteristics are associated with the development of epilepsies in the first year of life. We propose that one can better manage the clinical condition by identifying these brain morphological markers, including taking anticipatory measures.

All ZIKV-derived microcephaly populations displayed a lower incidence of rhombencephalic malformations in comparison to the prosencephalon [2-5]. Those findings are corroborated by the preservation of auditory processing in the brainstem [27]. Rhombencephalic abnormalities have been associated with a variety of neurological disorders [28], while mutations in the RELN gene are correlated with cerebellar hypoplasia and generalized epilepsy [29]. One possibility is that impaired brainstem and cerebellum development can lead both to the motor component of the spasms, derived from the decreased activity in pathways that control spinal reflex activity, and to the distinctive EEG discharge, like hypsarrhythmia,

resulting from defects in the ascending/regulatory pathways to the cortex [30]. However, we cannot affirm that those individuals with malformations in the brainstem and cerebellum have their epileptiform discharges generated in these regions. Another possibility is that rhombencephalon malformations in the ZIKV infected children with microcephaly are a sign that indicates a higher degree of ZIKV infection spread and causing abnormal activity in several areas. This hypothesis fits with the finding that children displaying IED in our cohort had lower total brain volume than the others (Fig. 5). Therefore, it is important to identify signs that can give physicians predictive power when examining new microcephaly cases.

Abnormalities in EEG activity are common in subjects with microcephaly derived from TORCHs. Riikonen [31] reported a group of individuals with infantile spasms caused by the congenital infection with one of multiple viruses and bacteria. EEG features, like hypsarrhythmia, interictal spikes, and SWD were found in subjects with infections by all the pathogens. This raised the question about the influence of concurrent infection with TORCHs on the reported findings. The prevalence of microcephaly in the state of Rio Grande do Norte state and elsewhere in Brazil was low prior to the ZIKV outbreak [32] and the mothers tested for other TORCHs did not have confirmation of recent infection. Therefore, TORCHs are unlikely to have contributed to the EEG alterations in the cohort described here. Contrarily, the CT findings are typical of congenital ZIKV infection [2-5, 33] and structural variability may contribute to distinct expression of epileptiform discharges. An earlier study described EEG abnormalities in 62% of subjects with CZVS (similar to the proportion described here), including unilateral and bilateral interictal spikes, hypsarrhythmia and abnormal slow oscillations [11]. Another study also described a wide variety of epileptiform discharges, including hypsarrhythmia, slow waves, and fast runs of 4–12 Hz (usually 6 Hz) [12]. However, none of those previous studies demonstrated the existence of correlations between clinical, structural, and electroencephalographic findings. Here we described two characteristics that are predictive for the occurrence of IED associated or not with clinical seizures: rhombencephalon malformation and reduced total brain volume.

An essential aspect of characterizing the ZIKV-derived microcephaly is to determine whether the aspects of brain functioning that are impaired are disruptive of the children's cognitive development. Sleep spindles evolve and mature in the firsts two years of life [34], and its occurrence has been associated with cognitive development [35]. Here we report that the occurrence of epilepsies in these subjects was associated with a reduced probability of developing sleep spindles. Moreover, we report the occurrence of a slower (6 Hz), spindle-shaped wave in the theta-band during sleep (supplementary Fig. 6). This atypical oscillation can indicate a malfunction in the circuitry responsible for generating proper sleep spindles. More investigation is needed to determine whether antiseizure medicine is capable of changing the occurrence of the 6-Hz oscillation and rescuing the expression of sleep spindles.

The interpretation of the data reported in this study has some limitations, however. First, our analysis was based on a small cohort of CZVS subjects from one single center at the Rio Grande do Norte state. It will be essential to verify whether the reported correlations between brain morphology and electrophysiological features stand for other populations. Also, we did not analyze the EEG profile in subjects older than 13 months of age. Therefore, we do not know whether epileptiform discharge delays the development of sleep spindles or abnormal sleep spindles is one of the electrophysiological hallmarks of CZVS. Although epilepsy incidence after the first year of life is low in CZVS [24], it is possible that the occurrence of epileptiform discharges hampers the maturation of sleep spindles in those subjects. Future studies with older populations will be necessary to verify the development of sleep spindle in this syndrome.

The present study describes a wide variety of electrophysiological findings in children with microcephaly associated with congenital ZIKV infection. In addition to the reduced rates of sleep spindles and the appearance of a 6-Hz oscillation (in the theta range), we also demonstrated a strong correlation between IED and specific brain malformations. These findings contribute to our understanding of the complexity of this heterogeneous syndrome and provide new evidence that morphological features can explain, at least in part, the occurrence of IED. Future studies with large cohorts and in different populations of ZIKV-derived microcephaly subjects will be essential to test the consistency of the correlations reported here and might contribute to anticipating the natural course of the syndrome.

### Authors contribution

EBS and CMQ conceived and designed research, analyzed and interpreted data and wrote the manuscript; SMBJ conducted serologic analysis; GOCM and MMN performed and scored CT scans; GOCM rendered volumetry; CRSM, NMRA, MB, and ANM collected clinical data and provided clinical care; ANM assessed the neurological status of the patients; EBS, AJR, ANM, and CMQ performed and supervised the EEG recordings; PSS and CMQ reviewed EEG recordings; AJR, SMBJ, ANM, PSS, and AKB contributed with additional analysis and further to the manuscript's writing. All authors revised drafts of the manuscript and approved the final version.

### Declaration of Interests

We declare no competing interests associated with this work.

### Acknowledgments

We would like to thank the technical support of the imaging service at Onofre Lopes University Hospital for assistance in the procedures in recording EEG activity from all the subjects. We also thank Jenefer Blackwell, Ph.D. (University of Cambridge and Western Australia) and Tarciso Velho, Ph.D. for their helpful comments on the final version of the manuscript, Daniel Takahashi, Ph.D. for statistical advice, and Débora Koshiyama and Ismael Pereira for library support, Karla Rocha for administrative support, and Grace Santana for secretarial support.

### Data sharing

All data are available upon reasonable request to the corresponding author, and it will be shared according to the standards of ethical policies regulating data sharing of human subjects.

### Supplementary materials

Supplementary material associated with this article can be found in the online version at doi:[10.1016/j.eclinm.2020.100508](https://doi.org/10.1016/j.eclinm.2020.100508).

### References

- [1] França GVA, Schuler-Faccini L, Oliveira WK, et al. Congenital Zika virus syndrome in Brazil: a case series of the first 1501 livebirths with complete investigation. *Lancet* 2016;388(10047):891–7.
- [2] Aragao MFV, Linden VVD, Brainer-Lima AM, et al. Clinical features and neuroimaging (CT and MRI) findings in presumed Zika virus related congenital infection and microcephaly: retrospective case series study. *BMJ* 2016;353:i1901.
- [3] Hazin AN, Poretti A, Di Cavalcanti Souza Cruz D, et al. Computed tomographic findings in microcephaly associated with Zika Virus. *N Engl J Med* 2016;374(22):2193–5.
- [4] Ramalho Rocha YR, Cavalcanti Costa JR, Almeida Costa P, et al. Radiological characterization of cerebral phenotype in newborn microcephaly cases from 2015 outbreak in Brazil. *PLoS Curr* 2016;8.

- [5] Soares de Oliveira-Szejnfeld P, Levine, Melo ASdO D, et al. Congenital brain abnormalities and Zika virus: what the radiologist can expect to see prenatally and postnatally. *Radiology* 2016;281(1):203–18.
- [6] Garcez PP, Loliola EC, Madeiro da Costa R, et al. Zika virus impairs growth in human neurospheres and brain organoids. *Science* 2016;352(6287):816.
- [7] Ledur PF, Karmirian K, Pedrosa C, et al. Zika virus infection leads to mitochondrial failure, oxidative stress and DNA damage in human iPSC-derived astrocytes. *Sci Rep* 2020;10(1):1218.
- [8] Alarcon A, Martinez-Biarge M, Cabañas F, Hernanz A, Quero J, Garcia-Alix A. Clinical, biochemical, and neuroimaging findings predict long-term neurodevelopmental outcome in symptomatic congenital cytomegalovirus infection. *J Pediatr* 2013;163(3):828–34 e1.
- [9] Mizrahi EM, Kellaway P. Characterization and classification of neonatal seizures. *Neurology* 1987;37(12):1837.
- [10] Nogueira de Melo A, Niedermeyer E. The EEG in infantile brain damage, cerebral palsy, and minor cerebral dysfunctions of childhood. In: Niedermeyer E, Lopes da Silva F, editors. *Electroencephalography: basic principles, clinical applications, and related fields*. 3rd edition Baltimore: Williams & Wilkins; 1993. p. 373–82.
- [11] Carvalho MDCG, Miranda-Filho DdB, van der Linden V, et al. Sleep EEG patterns in infants with congenital Zika virus syndrome. *Clin Neurophysiol* 2017;128(1):204–14.
- [12] Kanda PAM, Aguiar AAX, Miranda JL, et al. Sleep EEG of microcephaly in Zika outbreak. *Neurodiagn J* 2018;58(1):11–29.
- [13] Miranda-Filho DDB, Martelli CMT, Ximenes RADA, et al. Initial description of the presumed congenital Zika syndrome. *Am J Public Health* 2016;106(4):598–600.
- [14] Moura da Silva AA, Ganz JSS, Sousa Pds, et al. Early growth and neurologic outcomes of infants with probable Congenital Zika Virus Syndrome. *Emerging Infect Dis* 2016;22(11):1953–6.
- [15] Ashwal S, Michelson D, Plawner L, Dobyns WB. Practice parameter: evaluation of the child with microcephaly (an evidence-based review). *Neurology* 2009;73(11):887–97.
- [16] PAHO. Guideline for Zika virus disease and its complications. Washington, DC: Pan American Health Organization; 2016 [http://iris.paho.org/xmlui/bitstream/handle/123456789/28405/9789275118948\\_eng.pdf?sequence=1%20&isAllowed=y.%203](http://iris.paho.org/xmlui/bitstream/handle/123456789/28405/9789275118948_eng.pdf?sequence=1%20&isAllowed=y.%203). Accessed July 29, 2020.
- [17] Brasil SM, Ministério da Saúde, Secretaria de Vigilância em Saúde, Departamento de Vigilância das Doenças Transmissíveis. Protocolo de vigilância e resposta à ocorrência de microcefalia e/ou alterações do sistema nervoso central (SNC). Brasília: Ministério da Saúde; 2016 <http://portal.arquivos.saude.gov.br/images/pdf/2016/marco/24/Microcefalia-Protocolo-vigil-ncia-resposta-versao2.1.pdf>. Accessed July 29, 2020.
- [18] Fenton TR, Kim JH. A systematic review and meta-analysis to revise the Fenton growth chart for preterm infants. *BMC Pediatr* 2013;13(1):59.
- [19] Villar J, Ismail LC, Victora CG, et al. International standards for newborn weight, length, and head circumference by gestational age and sex: the newborn cross-sectional study of the INTERGROWTH-21st project. *Lancet* 2014;384(9946):857–68.
- [20] Papageorghiou AT, Ohuma EO, Altman DG, et al. International standards for fetal growth based on serial ultrasound measurements: the fetal growth longitudinal study of the INTERGROWTH-21st project. *Lancet* 2014;384(9946):869–79.
- [21] Holland D, Chang L, Ernst TM, et al. Structural growth trajectories and rates of change in the first 3 months of infant brain development. *JAMA Neurol* 2014;71(10):1266–74.
- [22] Real R, Vargas JM. The probabilistic basis of Jaccard's index of similarity. *Syst Biol* 1996;5(3):380–5.
- [23] Scheffer IE, Berkovic S, Capovilla G, et al. ILAE classification of the epilepsies: position paper of the ILAE commission for classification and terminology. *Epilepsia* 2017;58(4):512–21.
- [24] Carvalho M, Ximenes RAA, Montarroyos UR, et al. Early epilepsy in children with Zika-related microcephaly in a cohort in Recife, Brazil: characteristics, electroencephalographic findings, and treatment response. *Epilepsia* 2020;61(3):509–18.
- [25] Pereira H, Dos Santos SP, Amancio A, et al. Neurological outcomes of congenital Zika syndrome in toddlers and preschoolers: a case series. *Lancet Child Adolesc Health* 2020;4(5):378–87.
- [26] Ventura CV, Maia M, Bravo-Filho V, Góis AL, Belfort R. Zika virus in Brazil and macular atrophy in a child with microcephaly. *Lancet* 2016;387(10015):228.
- [27] Marques Abramov D, Saad T, Gomes-Junior S-C, et al. Auditory brainstem function in microcephaly related to Zika virus infection. *Neurology* 2018;90(7):e606–e14.
- [28] Barkovich AJ. Developmental disorders of the midbrain and hindbrain. *Front Neuroanat* 2012;6.
- [29] Hong SE, Shugart YY, Huang DT, et al. Autosomal recessive lissencephaly with cerebellar hypoplasia is associated with human RELN mutations. *Nat Genet* 2000;26(1):93–6.
- [30] Frost JD, Hrachovy RA. Pathogenesis of infantile spasms: a model based on developmental desynchronization. *J Clin Neurophysiol Off Publ Am Electroencephalogr Soc* 2005;22(1):25–36.
- [31] Riikonen R. Infantile spasms: infectious disorders. *Neuropediatrics* 1993;24(5):274–80.
- [32] Brasil, Governo do Estado do Rio Grande do Norte, Secretaria de Saúde Pública. Boletim epidemiológico: monitoramento dos casos de microcefalia e/ou alteração do sistema nervoso central no Rio Grande do Norte, Semana Epidemiológica 48 de 2019. Natal: subcoordenadoria de Vigilância Epidemiológica; 2019. <http://www.adcon.rn.gov.br/ACERVO/sesap/DOC/DOC000000000219921.PDF> [Accessed 29 July 2020].
- [33] Parra-Saavedra M, Reefhuis J, Piraquive JP, et al. Serial head and brain imaging of 17 fetuses with confirmed Zika Virus infection in Colombia, South America. *Obstet Gynecol* 2017;130(1):207–12.
- [34] Louis J, Zhang JX, Revol M, Debilly G, Challamel MJ. Ontogenesis of nocturnal organization of sleep spindles: a longitudinal study during the first 6 months of life. *Electroencephalogr Clin Neurophysiol* 1992;83(5):289–96.
- [35] Friedrich M, Wilhelm I, Molle M, Born J, Friederici AD. The sleeping infant brain anticipates development. *Curr Biol* 2017;27(15):2374–80 e3.